Technical Memorandum NESDIS 26

REMOVING STRIPES IN GOES IMAGES BY MATCHING EMPIRICAL DISTRIBUTION FUNCTIONS

Washington, D.C.
May 1989

UNITED STATES DEPARTMENT OF COMMERCE / National Oceanic and Atmospheric Administration / National Environmental Satellite, Data, and Information Service

NOAA TECHNICAL MEMORANDUMS

National Environmental Satellite, Data, and Information Service

The National Environmental Satellite, Data, and Information Service (NESDIS) manages the Nation's civil Earth-observing satellite systems, as well as global national data bases for meteorology, oceanography, geophysics, and solar-terrestrial sciences. From these sources, it develops and disseminates environmental data and information products critical to the protection of life and property, national defense, the national economy, energy development and distribution, global food supplies, and the development of natural resources.

Publication in the NOAA Technical Memorandum series does not preclude later publication in scientific journals in expanded or modified form. The NESDIS series of NOAA Technical Memorandums is a continuation of the former NESS and EDIS series of NOAA Technical Memorandums and the NESC and EDS series of the Environmental Science Services Administration (ESSA) Technical Memorandums.

These memorandums are available from the National Technical Information Service (NTIS), U.S. Department of Commerce, Sills Bldg., 5285 Port Royal, Springfield, VA 22161 (prices on request for paper copies or microfiche, please refer to PB number when ordering) or by contacting Nancy Everson, NOAA/NESDIS, 5200 Auth Road, Washington, DC 20233 (when extra copies are available). A partial listing of more recent memorandums appear below:

NESS 113 Satellite Indentification of Surface Radiant Temperature Fields of Subpixel Resolution. Jeff Dozier, December 1980. (PB81 184038)

NESS 114 An Attitude Predictor/Target Selector. Bruce M. Sharts, February 1981. (PB81 200479)

NESS 115 Publications and Final Reports on Contracts and Grants, 1980. Nancy Everson, June 1981. (PB82 103219)

NESS 116 Modified Version of the TIROS N/NOAA A-G Satellite Series (NOAA E-J) - Advanced TIROS-N (TN). Arthur Schwalb, February 1982. (PB82 194044)

NESS 117 Publications and Final Reports on Contracts and Grants, 1981. Nancy Everson, April 1982. (PB82 229204)

NESS 118 Satellite Observation of Great Lakes Ice - Winter 1979-80. Sharolyn Reed Young, July 1983. (PB84 101054)

NESS 119 Satellite Observation of Great Lakes Ice: 1980-81. A.L. Bell, December 1982. (PB83 156877)

NESDIS 1 Publications and Final Reports on Contracts and Grants, 1982. Nancy Everson, March 1983. (PB83 252528)

NESDIS 2 The Geostationary Operational Environmental Satellite Data Collection System. D.H. MacCallum and M.J. Nestlebush, June 1983. (PB83 257634)

NESDIS 3 Nimbus-7 ERB Sub-Target Radiance Tape (STRT) Data Base. L.L. Stowe and M.D. Fromm, November 1983. (PB84 149921)

NESDIS 4 Publications and Final Reports on Contracts and Grants, 1983. Nancy Everson, April 1984. (PB84 192301)

NESDIS 5 A Tropical Cyclone Precipitation Estimation Technique Using Geostationary Satellite Data. Leroy E. Spayd Jr. and Roderick A. Scofield, July 1984. (PB84 226703)

NESIDS 6 The Advantages of Sounding with the Smaller Detectors of the VISSR Atmospheric Sounder. W. Paul Menzel, Thomas H. Achtor, Christopher M. Hayden and William L. Smith, July 1984. (PB851518/AS)

NESDIS 7 Surface Soil Moisture Measurements of the White Sands, New Mexico. G.R. Smith, September 1984. (PB85 135754)

NOAA Technical Memorandum NESDIS 26

REMOVING STRIPES IN GOES IMAGES BY MATCHING EMPIRICAL DISTRIBUTION FUNCTIONS

M. P. Weinreb
Satellite Research Laboratory

R. Xie
Satellite Meteorological Center
Beijing, Peoples Republic of China

J. H. Lienesch
Satellite Research Laboratory

D. S Crosby
American University
Washington, D.C.

Washington, D.C.
May 1989

UNITED STATES
DEPARTMENT OF COMMERCE
Robert A. Mosbacher, Secretary

National Oceanic and
Atmospheric Administration
William E. Evans
Under Secretary

National Environmental Satellite,
Data, and Information Service
Thomas N. Pyke, Jr.
Assistant Administrator

National Oceanic and Atmospheric Administration
TIROS Satellites and Satellite Meteorology

ERRATA NOTICE

One or more conditions of the original document may affect the quality of the image, such as:

Discolored pages
Faded or light ink
Binding intrudes into the text

This has been a co-operative project between the NOAA Central Library and the Climate Database Modernization Program, National Climate Data Center (NCDC). To view the original document contact the NOAA Central Library in Silver Spring, MD at (301) 713-2607 x124 or Library.Reference@noaa.gov.

HOV Services
Imaging Contractor
12200 Kiln Court
Beltsville, MD 20704-1387
January 26, 2009

CONTENTS

TABLE

FIGURES

Removing Stripes in GOES Images by Matching Empirical Distribution Functions

M.P. Weinreb, R. Xie+, J.H. Lienesch, and D.S Crosby*
National Oceanic and Atmospheric Administration
National Environmental Satellite, Data, and Information Service
Washington, D.C. 20233

ABSTRACT. The current and future geostationary operational environmental satellites (GOES) of the National Oceanic and Atmospheric Administration (NOAA) are designed to produce visible images of the earth with linear arrays of eight detectors. Because the visible channels are not calibrated radiometrically in orbit, differences among instrument gains associated with the different detectors may cause artificial stripes to appear in the images. In the data processing on the ground, the images are "normalized" to remove the stripes. Images from future geostationary satellites, GOES I-M, will be normalized by the method of matching empirical distribution functions (EDF's). In this paper we report on a study of EDF matching with data from GOES-7. The technique was used to generate a normalization look-up table from data taken on May 18, 1988, and the table was applied to image data obtained two weeks later, on June 1, 1988. This successfully removed the stripes from the image. The severity of striping was assessed qualitatively from photographs of the images and quantitatively with numerical measures of striping derived from the EDF matching technique. The technique is expected to be even more effective with data from GOES I-M because of improvements in instrumentation.

1. INTRODUCTION

Both the current and future Geostationary Operational Environmental Satellites (GOES) of the National Oceanic and Atmospheric Administration (NOAA) are designed to carry instruments that image the full disk of the earth, or sections of it, in the visible region of the electromagnetic spectrum. Although they also image in the infrared region, the discussion in this paper will be confined to the visible. The current satellite, GOES-7 (Ensor, 1978), spins at 100 rpm on a north-south axis. Visible radiation is detected with an array of eight photomultipliers in a north-south line. The field of view from each photomultiplier is approximately 0.8 km square on the earth at the nadir. With each rotation of the satellite, eight parallel adjacent lines are swept out in the west-to-east direction. After each rotation a scan mirror is stepped to

---

+Permanent affilation, Satellite Meteorological Center, Beijing, Peoples Republic of China
*Permanent affiliation, The American University, Washington, D.C. 20016

displace the fields of view in the north-south direction. About 1800 steps are required to form a complete image of the earth. In the early 1990's, the GOES I-M system (Komajda and McKenzie, 1987), is expected to become operational. Instead of spinning, those satellites will be three-axis stabilized and will always present the same side to the earth. Each GOES I-M imager will utilize a linear array of eight detectors, which will be silicon photodiodes instead of photomultipliers. The field of view from a single detector will be approximately 1 km square on the earth at nadir. The imager will scan west-to-east and east-to-west by continuous movement of a plane mirror, and it will scan north-south by stepping the same mirror. Despite differences in instrumentation, the current and future GOES imagers have similar scanning geometries, which are depicted in fig. 1.

Henceforth, we will refer to each detector and its associated optics and signal-processing electronics as a channel. Each imaging instrument is then said to have eight visible channels. When stimulated with incident radiation, each channel responds with an output, measured in digital counts. We use the term "gain" to refer to the ratio of the change in the count output to the change in intensity of the incident radiation. The gain depends on the transmissivity of the optics, the responsivity of the detector, the amplification of the electronics, and the analog-to-digital conversion factor, among other things. When the instrument is in orbit, changes in gain, caused by changes in any of those sources, may occur.

In many systems, the output is a linear function of the incident intensity. Then the gain is independent of the incident intensity, and the instrument (or channel) is said to be linear. The visible channels of the GOES I-M imagers are designed to be linear. However, the visible channels of GOES-7 are not linear. This is by design, and is in addition to any unintended nonlinearity. In the analog-to-digital conversion, the output is made approximately equal to the square root of the incident intensity to take advantage of the increased sensitivity of the photomultipliers at low intensity levels (Ensor, 1978; Bristor, 1975). Therefore, the gain is a decreasing function of intensity. (The photomultipliers, which typically operate in a slightly nonlinear fashion, may also add to the nonlinearity.)

Once a GOES is in orbit, its visible channels cannot be calibrated radiometrically, because there is no calibrated source of visible radiation on board. This will also be the case for GOES I-M. One of the disadvantages of this is that since the gains (and offsets) of the eight channels may not all be equal and may change in time, artificial east-west stripes may appear in the images. Figure 2 shows striping in an image from GOES-7. Striping may also affect images from GOES I-M, although it is expected to be less severe. One reason for this is that the photodiode detectors of GOES I-M are expected to be more nearly uniform in their behavior and more stable in time than the photomultipliers of GOES-7. Also, the data from GOES I-M will be digitized more finely. The GOES-7 visible data are packaged in six-bit words. This will be increased to ten bits on GOES I-M. The more bits per word, the less significant the striping from quantization error.

In operational data processing at NOAA's National Environmental Satellite, Data, and Information Service (NESDIS), we compensate for channel-to-channel differences in gain with a procedure called normalization, which is applied to

the data with look-up tables. It is done automatically, continuously, and in real time at the ground station at Wallops, VA, as the data are received from the satellites and then retransmitted to users. Look-up tables are generated off line (and not in real time) in the main-frame computers at Suitland, MD. For each satellite instrument, a single table is applied to all image data from the entire disk of the earth. Because characteristics of the instruments change with time, new look-up tables are generated occasionally, usually once a week or less often. The current method of generating the operational look-up tables (J. Lienesch, NOAA/NESDIS, personal communication, 1980) has been in use since the mid-1970's. However, NESDIS plans to apply a different method, namely, the matching of empirical distribution functions (EDF's), to generate the tables for GOES I-M, because it is more efficient.

Matching of EDF's is a standard statistical technique and has already been applied to satellite data from the Landsat Multispectral Scanner (MSS) (see, e.g., Horn and Woodham (1979)). In that work, a normalization look-up table is derived and applied to the same sector of image data. Our application is different, however, because we are required to derive a table from a single "dependent" sector on a particular day and apply it for weeks afterwards to independent image data from all over the earth's disk.

In preparation for the launch of GOES I, we have been studying the feasibility of the EDF matching technique by applying it to data from GOES-7, which was the only multi-channel satellite imager whose data were conveniently available to us. Data from GOES-7 provide a severe test of the method, because it is expected that the data from GOES I-M will be easier to normalize than the data currently available from GOES-7, as we explained in previous paragraphs. This paper reports the results from our study.

2. THEORY

The basic premise of normalization is that if several channels view the same scene, their outputs should be equal, and this should be the case regardless of how bright the scene is. In actual application, no two channels ever view the same scene. Instead, we assume that with a large ensemble of measurements, the distribution of the intensity of the earth radiation incident on each detector will be similar (Horn and Woodham, 1979). (The distributions will not be identical, but the larger the ensemble, the more similar they will become.) With that assumption, the basic premise becomes that the distributions of the outputs of each channel should be identical.

In our approach, we designate one of the channels as a reference channel. Then the outputs of the other channels are adjusted so that their distributions are the same as that of the reference channel. A reference channel should meet certain criteria. When it views the earth, its outputs should fill as much of the dynamic range of the data system as possible without clipping at either the low or high ends. Also, a reference channel should have low noise and a stable gain, one that does not change rapidly with time. Because the characteristics of the silicon photodiode detectors of GOES I-M are expected to be stable in time, a particular channel may be usable as the reference for years, and a single normalization look-up table may be effective for months.

To generate a normalization look-up table, we begin by selecting a sample of full-resolution unnormalized earth-scene data covering as much of the range of intensities as possible. For GOES I-M, the area will be rectangular, extending several thousand pixels both east to west and north to south. Corresponding to the incoming radiance from any pixel, the instrument will respond with an output x, in digital counts. One can compile the discrete density function, i.e., the histogram, describing the relative frequency of occurrence of each possible count value, for each channel. For channel i, which is the channel to be normalized, let the histogram be $p_i(x)$. An empirical distribution function (EDF) $P_i(x)$ can then be generated; viz.,

$$P_i(x) = \sum_{t=0}^{x} p_i(t).$$

The EDF is also known as a cumulative histogram of relative frequency. It is a non-decreasing function of x, and its maximum value is unity. For convenience, however, we have chosen the maximum value to be 100%; i.e., if the maximum possible output in counts is X, then

$$P_i(X) = 100\%.$$

In these terms, the basic premise of normalization is that for each output value x in channel i, the normalized value x' should satisfy

$$P_r(x') = P_i(x), \tag{1}$$

where the subscript r refers to the reference channel. In practice, not only is P_r nondecreasing, but it is also monotonically increasing as a function of x' in the domain of x' where there are data. Therefore, it can be inverted, yielding the solution for x',

$$x' = P_r^{-1}(P_i(x)). \tag{2}$$

When it is applied sequentially for every possible count value x, eq.(2) generates the normalization look-up table relating each x to an x'. Figure 3 depicts how the procedure is applied in actual practice to generate one entry in the table. (Also see Horn and Woodham (1979).) The figure depicts idealized EDF's for the reference channel and channel i. In the figure the EDF's are continuous, but in practice they are discrete, being specified only at integer values of x. To find x_1', the normalized count value corresponding to the observed count value of x_1, the following is the procedure: First, for the count value x_1 in channel i, find the percentage value from the EDF of channel i. In the illustration it is $P_i(x_1)$. Then find the point on the reference channel's EDF with the same percentage value. According to eq.(1), that percentage can also be expressed as $P_r(x_1')$. Finally, use the EDF of the reference channel to find the normalized count value x_1'. Since the data are actually discrete, we will need to interpolate within the EDF of the reference channel to find the value of x_1', which must then be rounded to the nearest integer.

This technique not only generates the normalization look-up table, but it also provides yardsticks to measure the severity of striping. Striping exists

when the EDF's of channel i and the reference channel are not identical. The distances between them, along either the abscissa or the ordinate in fig. 3, measure the degree of striping. Henceforth, these distances will be called count differences and percent differences, respectively. In the terminology of eq. (2), the count differences are $x - x'$, and the percent differences are $P_i(x) - P_r(x)$.

3. RESULTS AND DISCUSSION

A normalization look-up table was generated from a dependent sample consisting of unnormalized data from GOES-7 on May 18, 1988. The table was applied to normalize an independent sample of image data from GOES-7 two weeks later, on June 1, 1988. Both samples were produced at the same time of day, approximately 1400 EDT (1800Z), when the disk of the earth beneath the satellite was in full sunlight.

3.1 Generation of normalization look-up table

The dependent sample consists of unnormalized data from all pixels in a rectangular sector 1996 pixels east-west and 2400 pixels north-south, located near the equator, as depicted in fig. 4. An image of approximately 15% of that sector appears in fig. 2, and, as we had pointed out previously, it is striped. The striping is most severe at the mid- and high-intensity levels (low and high cloud), which appear gray and white, respectively, in the photograph.

For each of the channels, histograms were compiled from the data in the full dependent sample. Each histogram represents GOES-7 output data from 598,800 (=1996 x 300) pixels. The three panels in fig. 5 show the histograms for channels 2, 5, and 6. The abscissae, labelled "Intensity (Counts)", are the output levels, and the ordinates, labelled "Frequency", are the frequencies of occurrence of the outputs at each level. Based on the criteria mentioned previously, channel 2 was designated as the reference. We chose channels 5 and 6 as examples because of all the channels their histograms are the most different from the reference channel's. The histogram of channel 5 is displaced towards the high intensities relative to that of the reference channel, and its upper end is clipped. It is also broader than the reference channel's, indicating that the gain in channel 5 is greater overall than that of the reference channel. With channel 6, the situation is reversed. The histogram is shifted towards the lower intensities. Also, it is compressed relative to the histogram of the reference channel, and the data do not fill the dynamic range of the data system, indicating that the gain in this channel is lower overall than that in the reference channel. All three histograms are somewhat similar in shape; i.e., each channel has a high frequency of occurrence of low-level outputs, which correspond primarily to ocean areas, and a decrease in frequency with increasing intensity. However, the size of the secondary peak at the high-intensity end, corresponding to high clouds, differs from channel to channel, and it is missing entirely for channel 6. This suggests that the dependence of gain on intensity (or the degree of nonlinearity) varies from channel to channel.

Figure 6 shows the EDF's of channels 5 and 6, as well as the EDF of channel 2, the reference channel, which were computed from the histograms in fig. 5.

The abscissa, labelled "Intensity (Counts)", is the output level, and the ordinate, labelled "Percentile", is the percentage of the data with outputs at or below that level.

We applied eq. (2) to these EDF's and those of the other channels to generate the normalization look-up table, which is presented in the Appendix. It can be seen that the tabulated relationships between raw and normalized counts differ from channel to channel, and some of them are nonlinear. This is symptomatic of the differences in the dependence of gain on intensity among the channels.

3.2 Application to independent sample

The independent sample of unnormalized GOES -7 data was produced on June 1, 1988, from a sector of 1996 x 2400 pixels located near the top of the globe, as depicted in fig. 4. An image of approximately 15% of that sector is shown in fig. 7. Again, there is striping, and it is most severe at the mid- and high-intensity levels. Figure 8 shows the histograms compiled in each of channels 2, 5, and 6. Like the histograms of May 18, they show channel-to-channel differences in position and width, and they are again similar to each other in shape. However, their shapes are unlike those of the May 18 histograms, due to the difference in location of the two images and the difference in the distribution of clouds.

The EDF's for channels 2, 5, and 6 are plotted in fig. 9. They are shaped differently from the EDF's of May 18. However, for the May 18 normalization look-up table to be effective on June 1, the channel-to-channel relationships among the EDF's must be similar on the two dates; i.e., the relative (channel to channel) gain functions must be similar. Although it may not be obvious here, the results below demonstrate that this is in fact the case.

We normalized the data from June 1 by applying the May 18 look-up table, which is listed in the Appendix. Figure 10 shows the histograms of the normalized data for channels 5 and 6. In position and shape they are now much more like the histogram of the reference channel, which is reproduced in the upper panel for comparison. An interesting feature of these histograms is the presence of breaks; i.e., intensity levels with a zero frequency of occurrence. Breaks are caused by discontinuities, i.e., missing intensity levels, in the look-up tables. For example, the histogram for channel 6 has a break at the 21-count level, and there is a corresponding discontinuity in the look-up table at that level. Breaks and discontinuities are the result of the round-off required when the tables are generated from discrete data. Note also that breaks are especially prevalent in the histogram of channel 6. For this channel, the original histogram is compressed relative to the reference channel's, so the normalization procedure must stretch it out. With discrete data, this causes breaks. (The process may be visualized as the breaking of a "brittle" histogram under tension.) An interesting question is why breaks also occur in the histogram of channel 5, which the normalization procedure compressed overall. The explanation is that there are limited regions in the histogram where it was stretched.

Figure 11 shows the EDF's of the normalized data for all three channels. Normalization has made the differences among them practically insignificant.

(The EDF's of the other five channels behave similarly.) The largest differences occur where the EDF's of channel 5 or 6 have steps, or flat spots. These are caused by the breaks in the histograms and are, therefore, an artifact of digitization.

Figure 12 is the normalized image of the same area as was shown in fig. 7. It is the "after" to the "before" of fig. 7. The improvement is obvious, since the normalized image has no stripes.

As a quantitative measure of the striping, we had previously proposed the differences, expressed in counts or in percent, between the EDF of the reference channel and those of each of the other channels. The count differences for the unnormalized (raw) data of June 1 are plotted in fig. 13 (open symbols) for channels 5 and 6. (A few points are missing at the low and high intensity ends, where there are no data.) In the terminology of eq. (2) and fig. 3, these are plots of $x - x'$ vs x.

Figure 13 shows that, for the unnormalized data, the differences between the EDF of the reference channel and the EDF's of channels 5 and 6 are substantial, which is consistent with the severity of striping seen in the unnormalized image (fig. 7). In addition, it shows that those differences are not linear functions of intensity. In other words, relative to that of channel 2, the output vs incident intensity functions in channel 5 and 6 are nonlinear.

The count differences in channels 5 and 6 for the normalized data of June 1 are also shown in fig. 13 (solid symbols). (The figure has no points at intensity levels where breaks occur in the histograms or near the low and high intensity ends, where there are no data.) Normalization generally reduced all the count differences to 0 or 1 unit in magnitude. The sole exceptions are the values of -2 in both channels at the one-count level, but they are hardly significant, since practically no data are involved--only three pixels in channel 5 and one in channel 6. The count differences in all the other channels are equally small, consistent with the lack of striping seen in the image (fig. 12).

The differences expressed in percent are plotted in fig. 14--open symbols for the unnormalized (raw) data, and solid for the normalized data. In the terminology of eq. (2) and fig. 3, the plots in fig. 14 are of $P_i(x) - P_r(x)$ vs x. Normalization reduced the percent differences substantially. Note that in absolute value the percent differences tend to be large when the slopes of the EDF's are large. For the unnormalized data there are two such regions, which occur near 16 and 42 counts for channel 5 and near 12 and 34 counts for channel 6. By the same token, the relatively large differences in the normalized data near the 12-count level correspond to the positions of steepest slopes in the normalized EDF's.

Figures 11, 13, and 14 all indicate that the normalization was successful in making the EDF's of the three channels nearly identical. This implies that the relationships among the EDF's remained essentially the same between May 18 and June 1, as was surmised in an earlier paragraph, despite the changes in the images and the EDF's themselves. Those relationships, in fact, depend only on the relative gains and offsets among the channels. As long as the relative gains and offsets remain the same, the normalization look-up tables remain

effective. Although we do not show the results here, we found that the effectiveness of the May 18 normalization look-up tables decreased only slightly with time over a six-week period. After six weeks, the count differences in the normalized data were still either zero or one unit at most intensity levels, the only exception being the emergence of a two-unit count difference at two intensity levels in channel 6. Therefore, any changes in relative gains and offsets, which, e.g., might have resulted from seasonal variation of temperatures on the satellite, had to be small over the period.

4. CONCLUSION

This paper presents a case study in which a normalization look-up table generated from GOES-7 data of May 18, 1988, removed the stripes from an image obtained on June 1, 1988. This is strong evidence that normalization by EDF matching is an effective method for removing striping from visible images from GOES.

The severity of the striping was determined qualitatively from photographs of the images and quantitatively with numerical measures of striping--the empirical distribution functions themselves and the count and percent differences among them.

The method worked despite the nonlinearities in the outputs of the GOES-7 visible channels and the substantial nonuniformities in gain. We expect it to work at least as well with data from GOES I-M, because the responses in the GOES I-M channels are expected to be linear and more nearly uniform than those of GOES-7. Furthermore, we found that the same normalization table remained effective for at least six weeks. Since the gains of the GOES I-M channels are expected to be more stable in time than those of GOES-7, we would expect a normalization table to remain valid for even longer periods with GOES I-M.

ACKNOWLEDGMENTS

The authors are indebted to Dong Han of NOAA/NESDIS for providing the raw image data; to Gene Legg of NOAA/NESDIS for producing the "sectorizer" images that appear in figs. 2, 7, and 12; to Donald Mack of Integral Systems, Inc., of Lanham, MD, for supplying information on the application of EDF matching to data from Landsat; and to George Jones and Paige Bridges of NOAA/NESDIS for preparing the figures.

REFERENCES

Bristor, C. L. (Ed.) (1975), Central processing and analysis of geostationary satellite data, NOAA Tech. Mem. NESS 64, National Oceanic and Atmospheric Administration, National Environmental Satellite Service, Washington, DC, 155 pp.

Ensor, G. J. (1978), User's guide to the operation of the NOAA geostationary satellite system, U.S. Department of Commerce, National Oceanic and Atmospheric Administration, National Environmental Satellite Service, Washington, DC, October 1978, 101 pp.

Horn, B. K. P. and Woodham, R. J., (1979), Destriping LANDSAT MSS images by histogram modification, Computer Graphics and Image Processing 10:69-83.

Komajda, R. J. and McKenzie, K., (1987), An introduction to the GOES I-M imager and sounder instruments and the GVAR retransmission format, NOAA Tech. Rep't. NESDIS 33, National Oceanic and Atmospheric Administration, National Environmental Satellite, Data, and Information Service, Washington, DC, 51 pp.

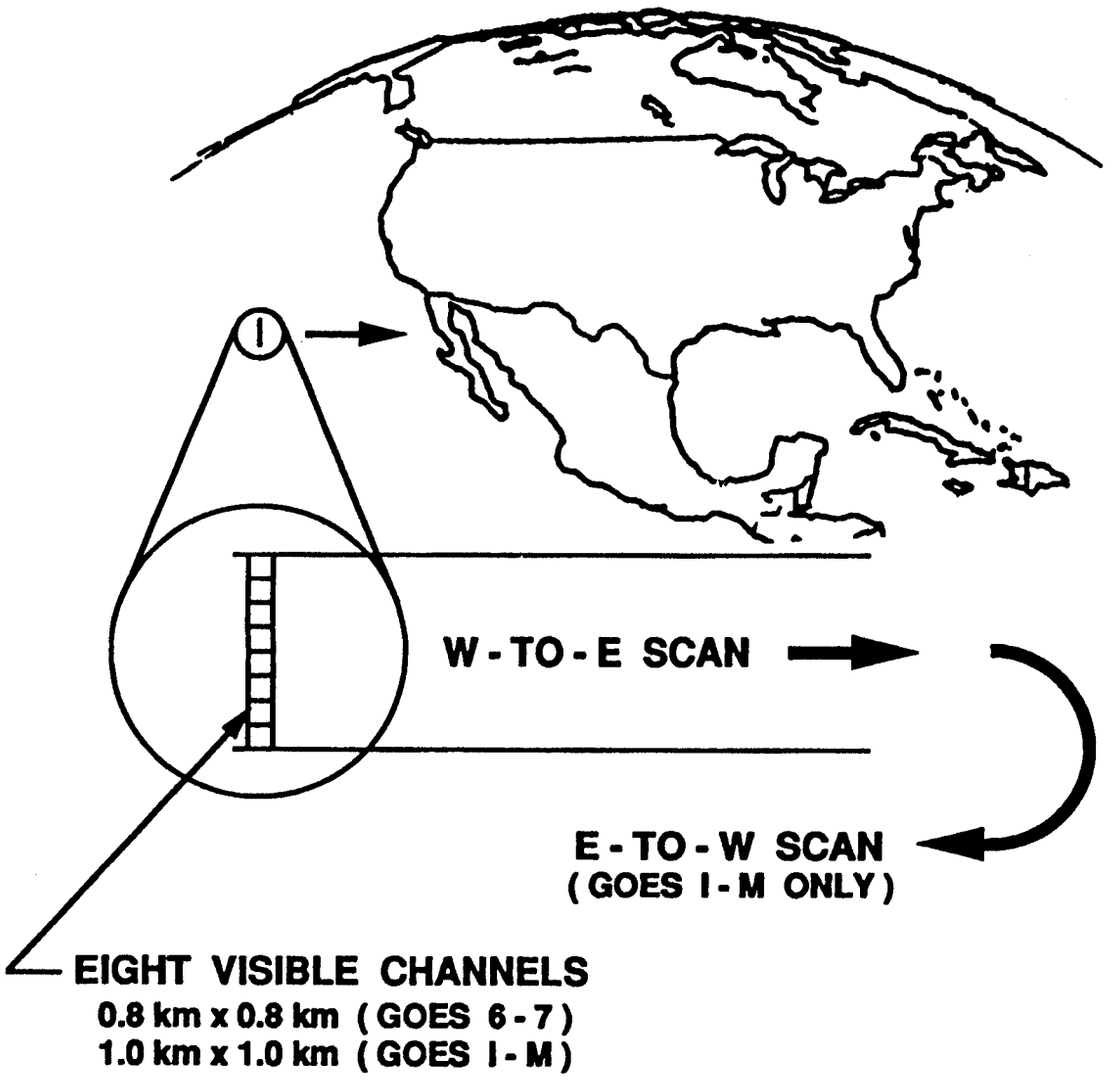

FIGURE 1. Scanning geometry of GOES imagers.
(Not to scale)

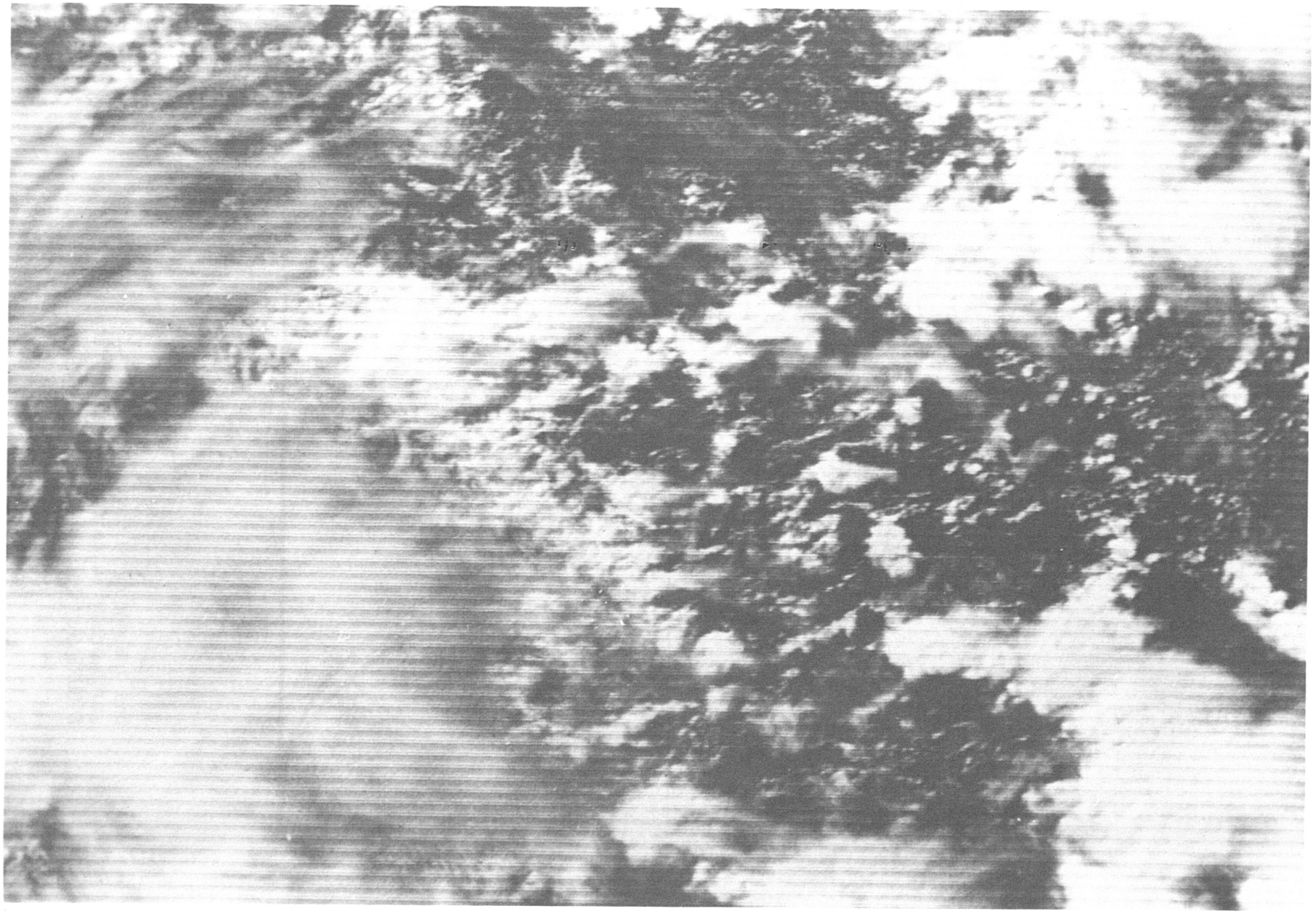

FIGURE 2. Unnormalized GOES-7 image, May 18, 1988.

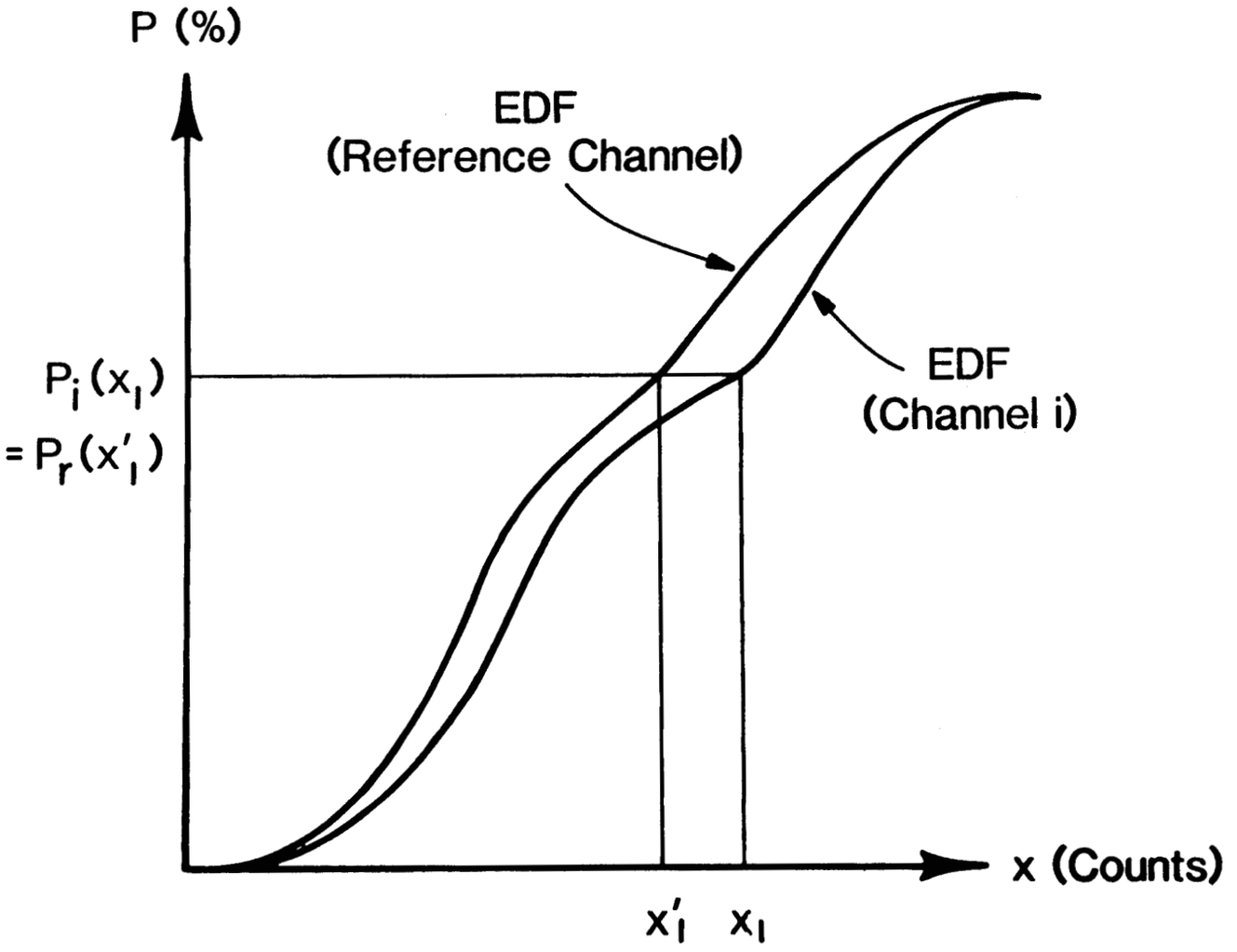

FIGURE 3. Illustration of procedure to generate normalization look-up table (see text for explanation).

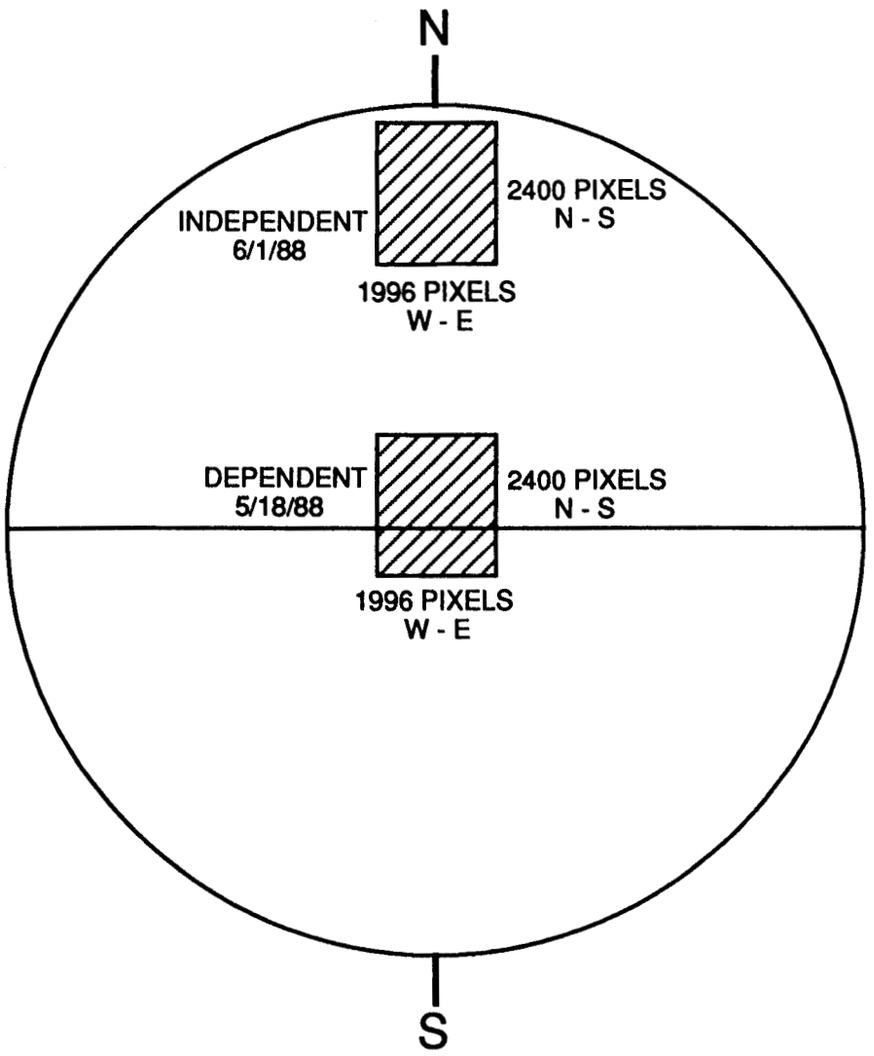

FIGURE 4. Location on globe of dependent and independent samples of image data, 1996 x 2400 pixels.

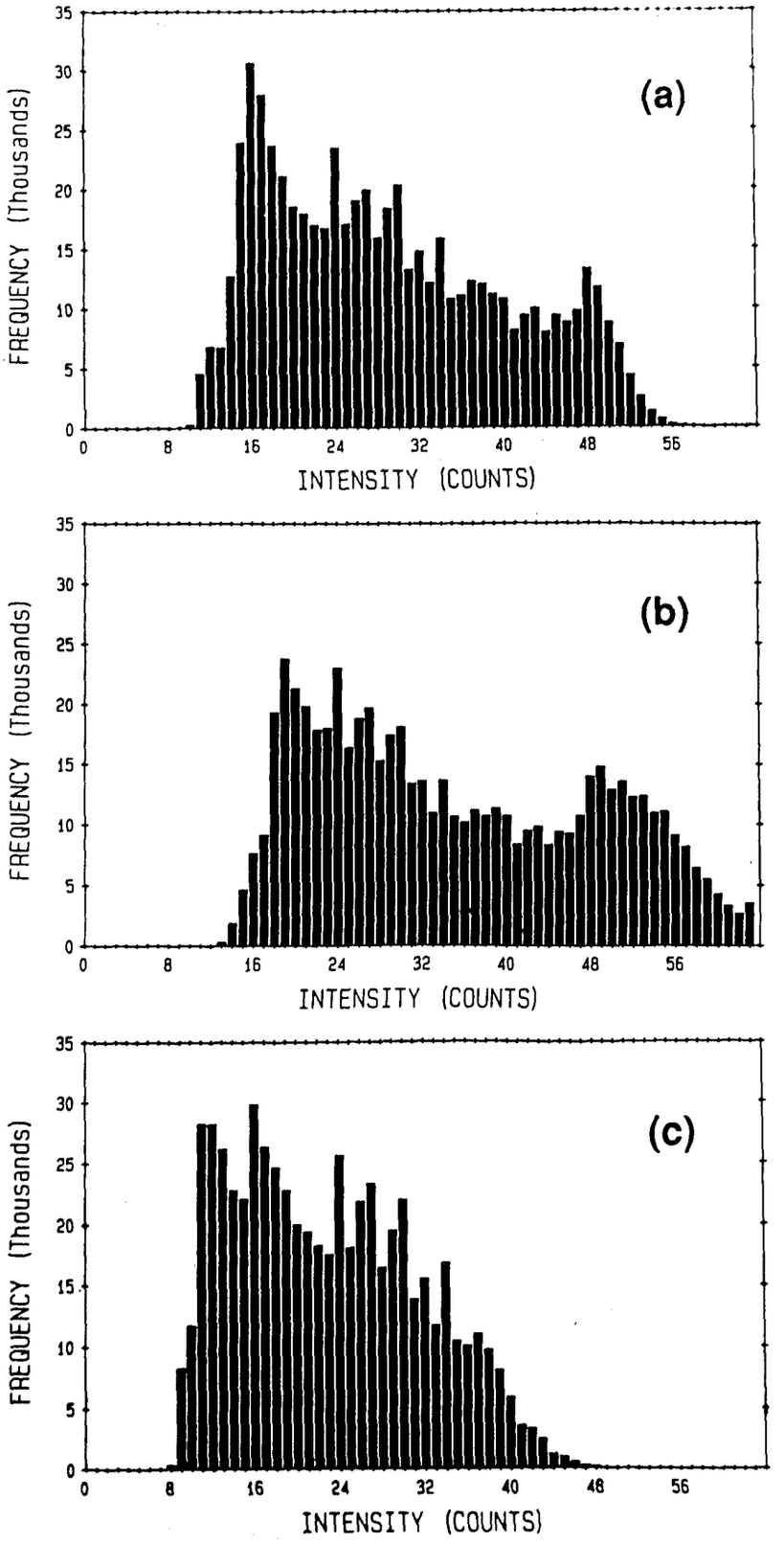

FIGURE 5. Histograms of unnormalized GOES-7 image data, May 18, 1988. (a) Channel 2. (b) Channel 5. (c) Channel 6.

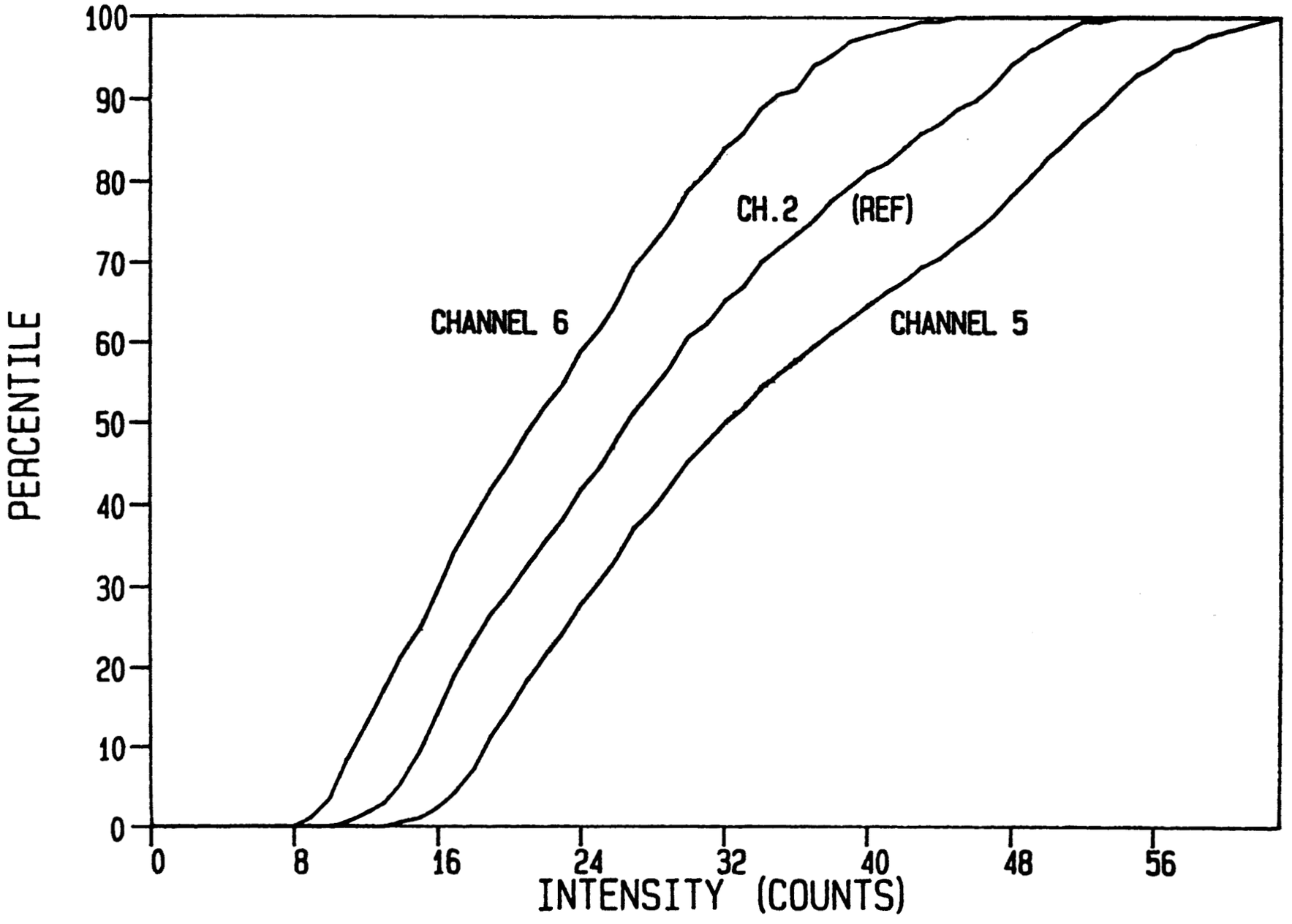

FIGURE 6. Empirical distribution functions for unnormalized GOES-7 image data, May 18, 1988.

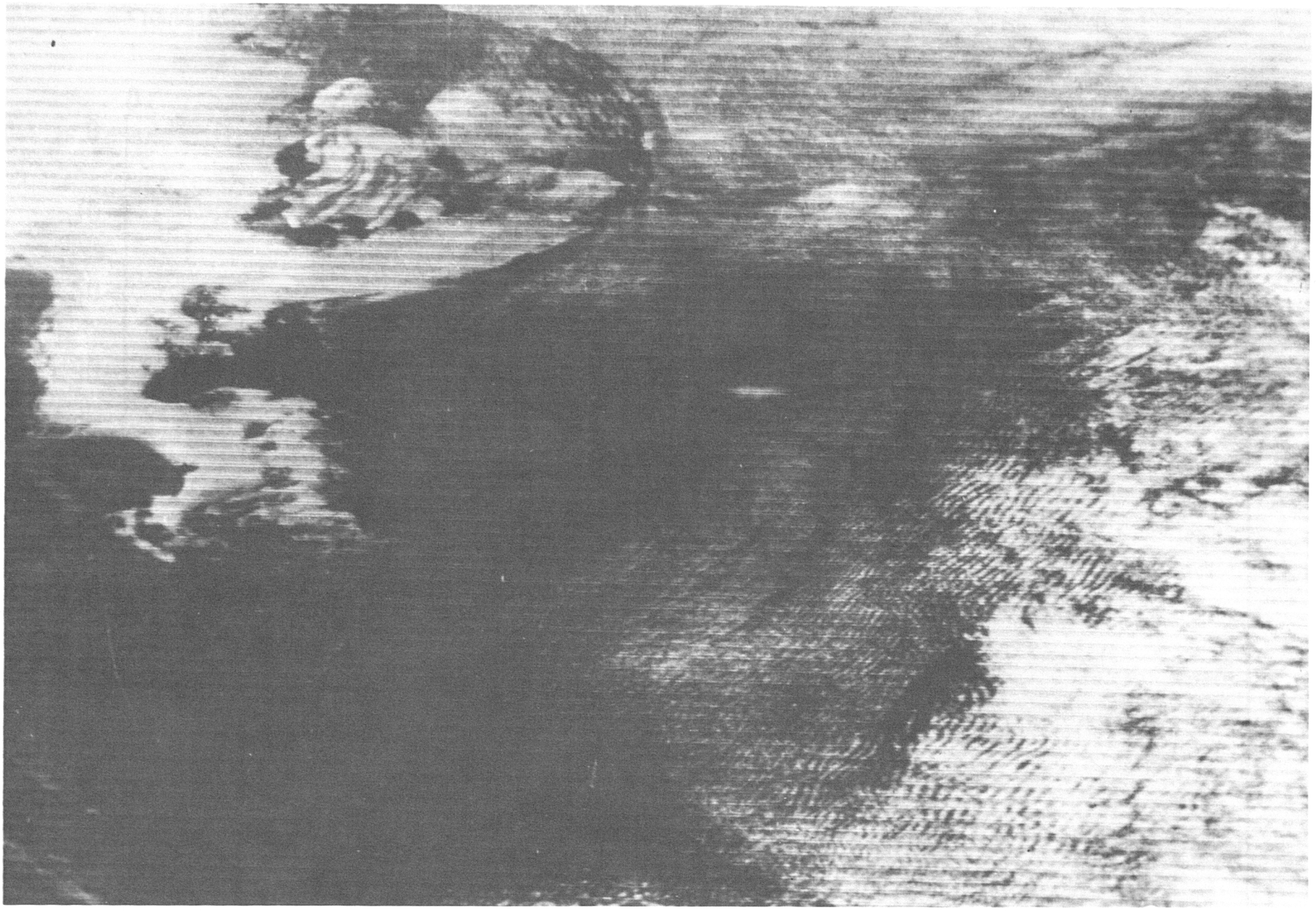

FIGURE 7. Unnormalized GOES-7 image,
June 1, 1988.

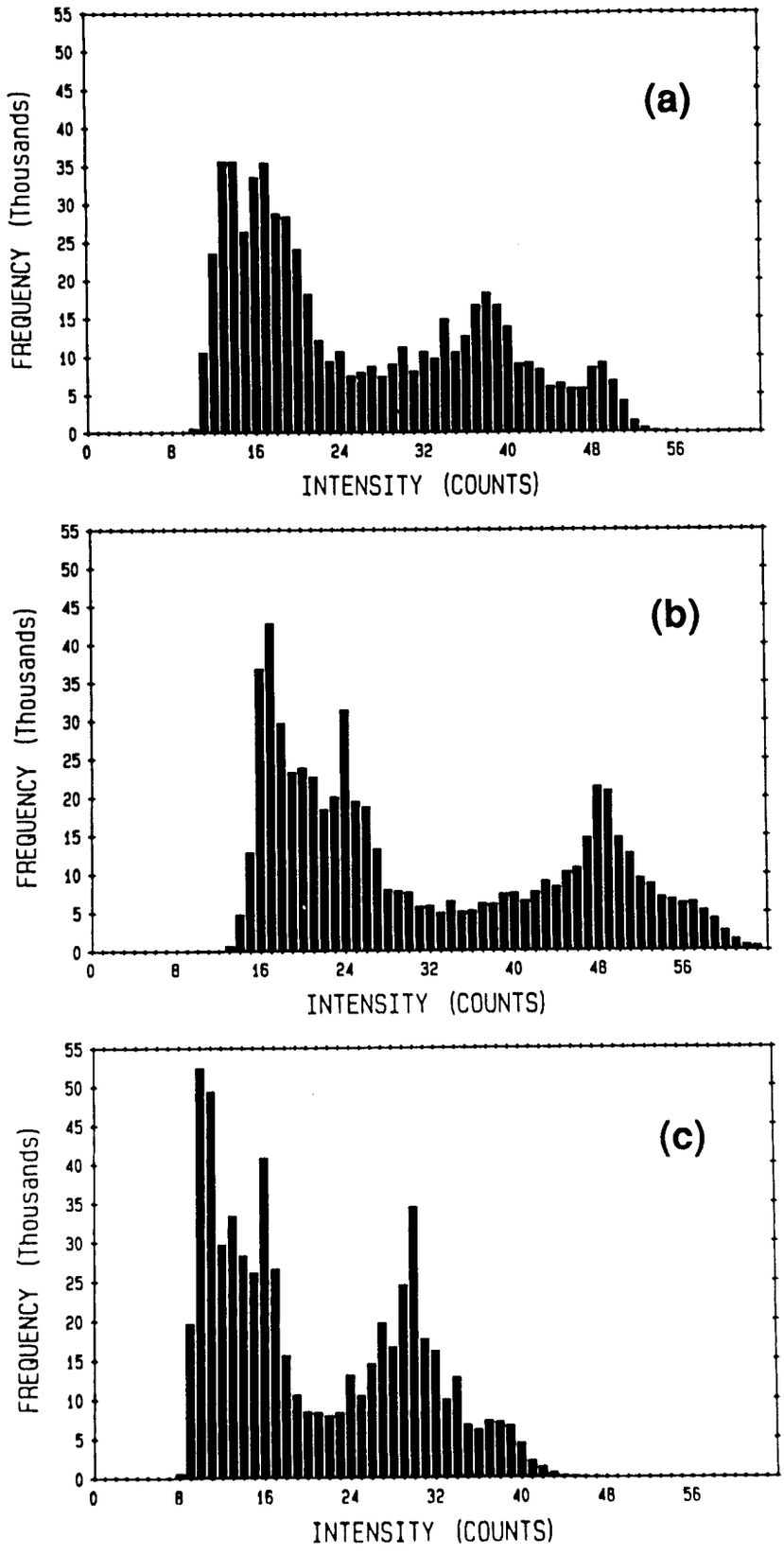

FIGURE 8. Histograms of unnormalized GOES-7 image data, June 1, 1988. (a) Channel 2. (b) Channel 5. (c) Channel 6.

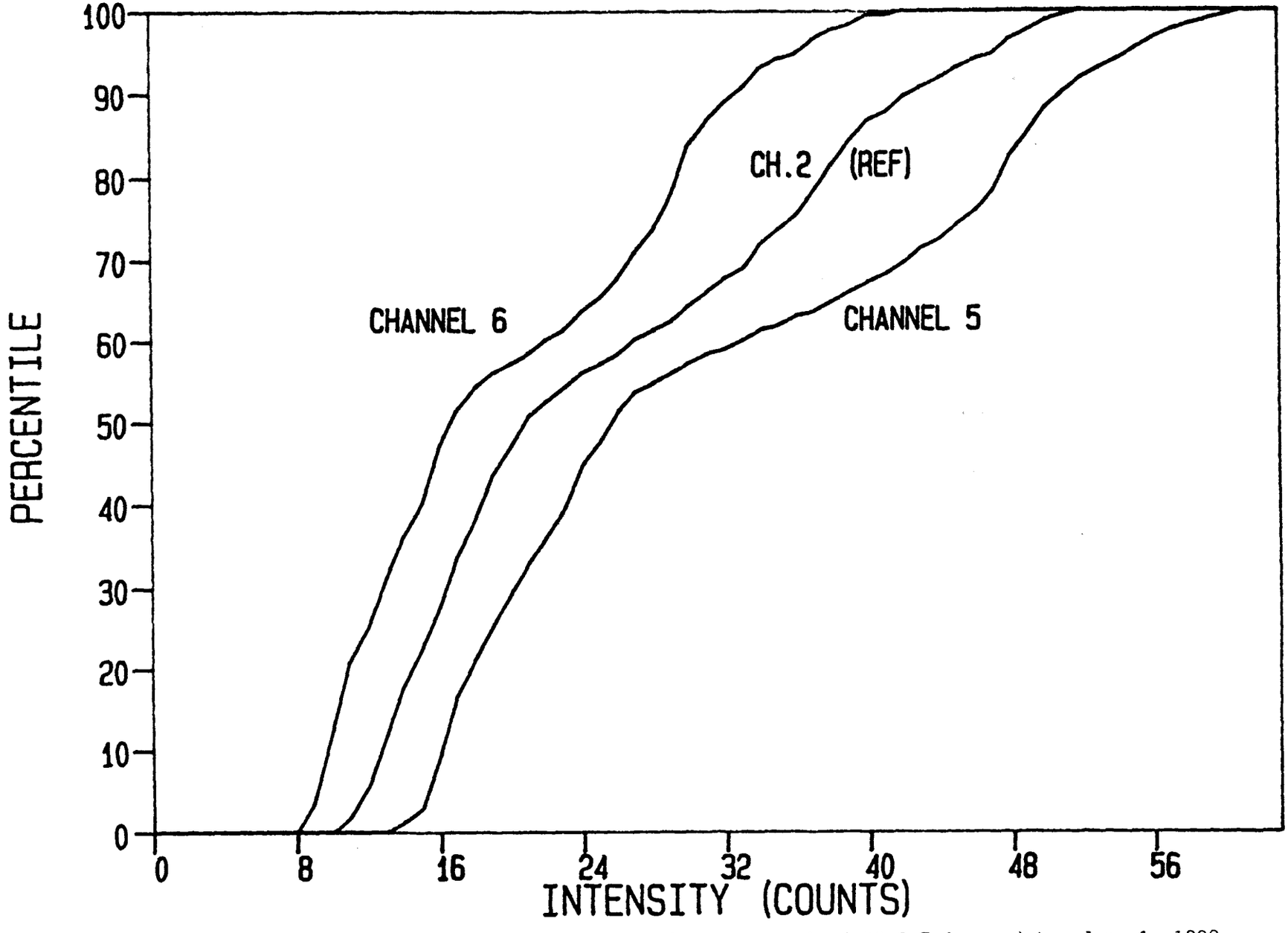

FIGURE 9. Empirical distribution functions for unnormalized GOES-7 image data, June 1, 1988.

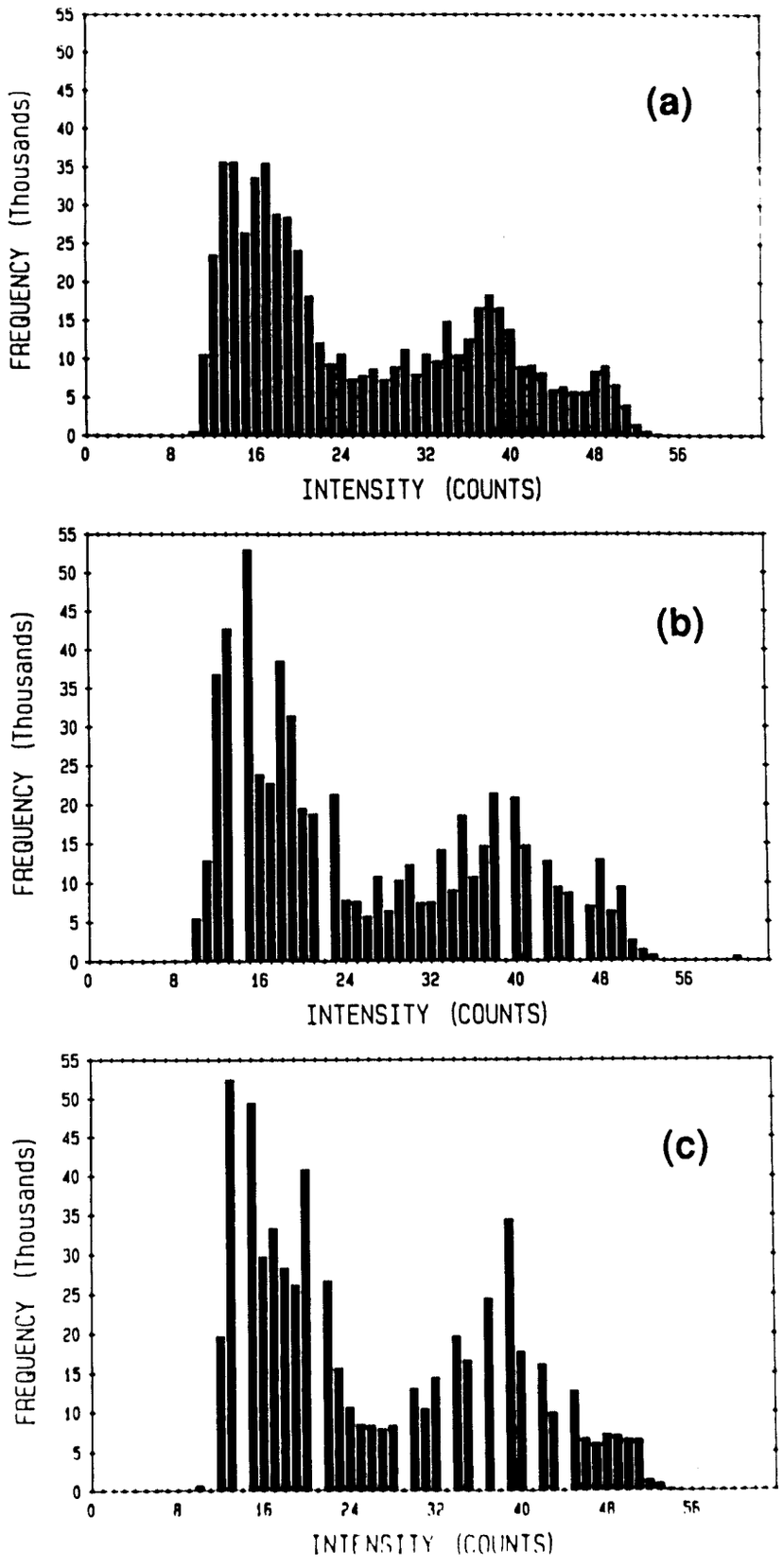

FIGURE 10. Histograms of normalized GOES-7 image data, June 1, 1988. (a) Channel 2. (b) Channel 5. (c) Channel 6. (Data in Channel 2, the reference channel, are never normalized.)

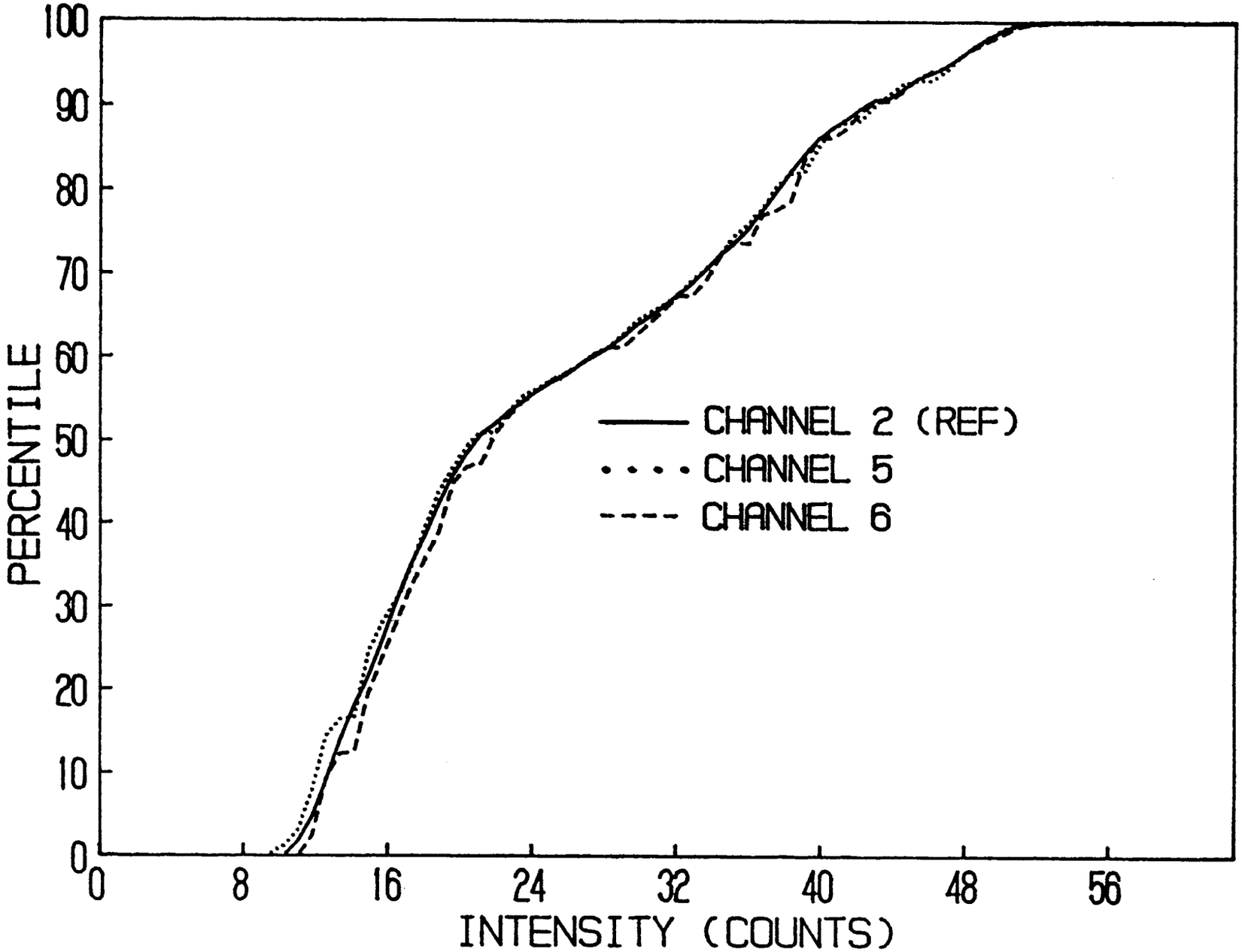

FIGURE 11. Empirical distribution functions for normalized GOES-7 data, June 1, 1988. (Data in Channel 2, the reference channel, are never normalized.)

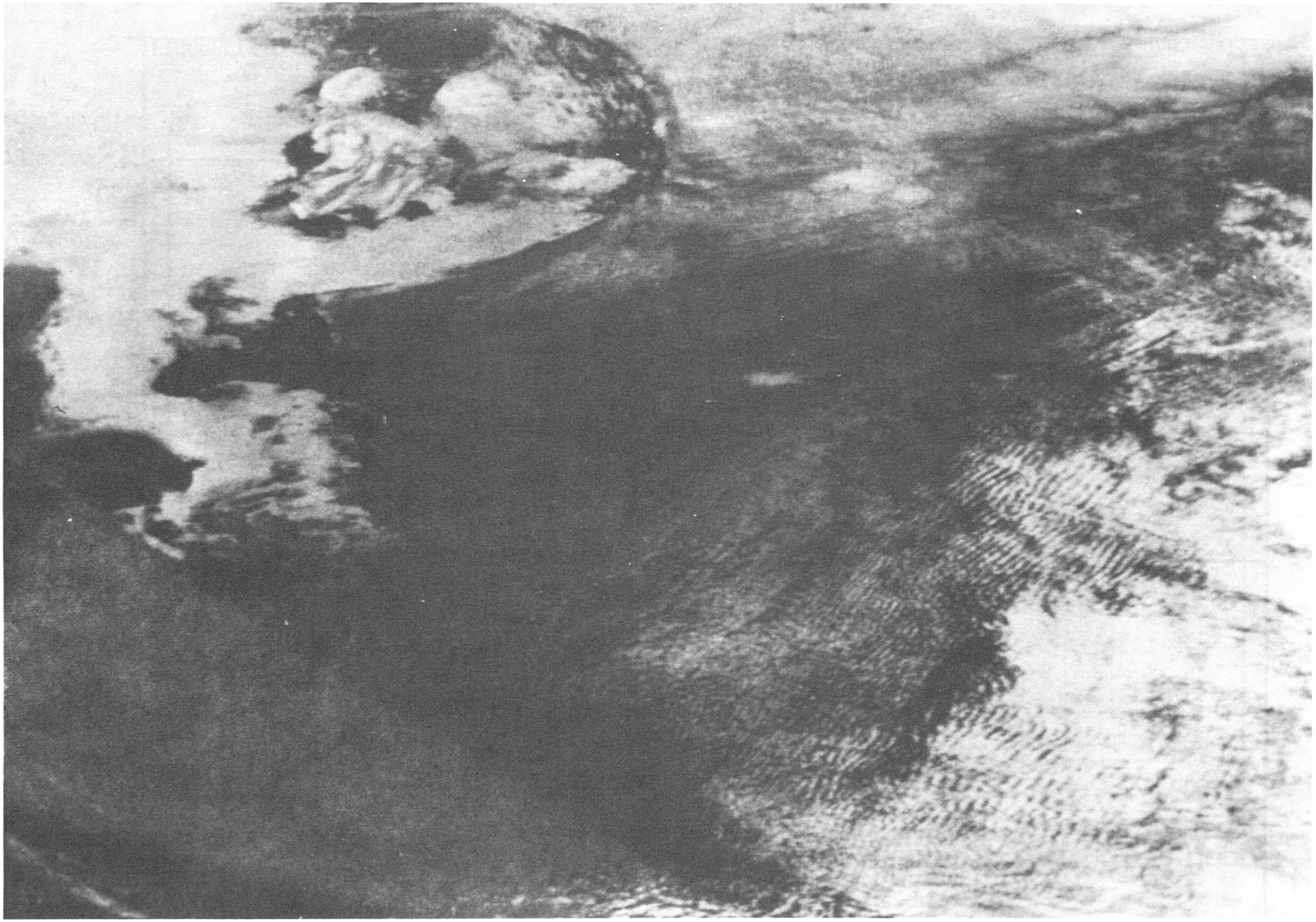

FIGURE 12. Normalized GOES-7 image, June 1, 1988.

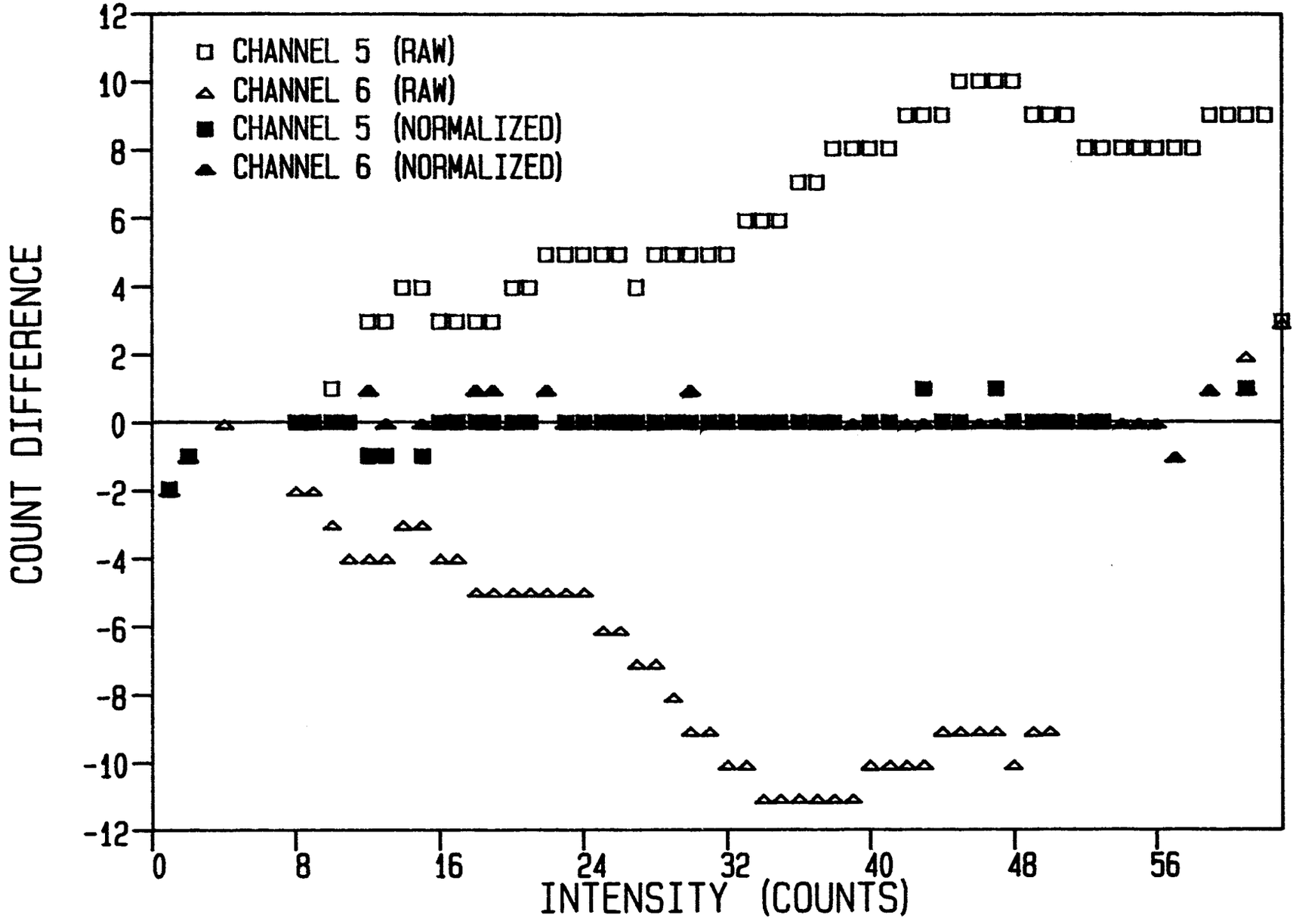

FIGURE 13. Count differences for image data of June 1, 1988. Open symbols indicate unnormalized (raw) data; solid, normalized data.

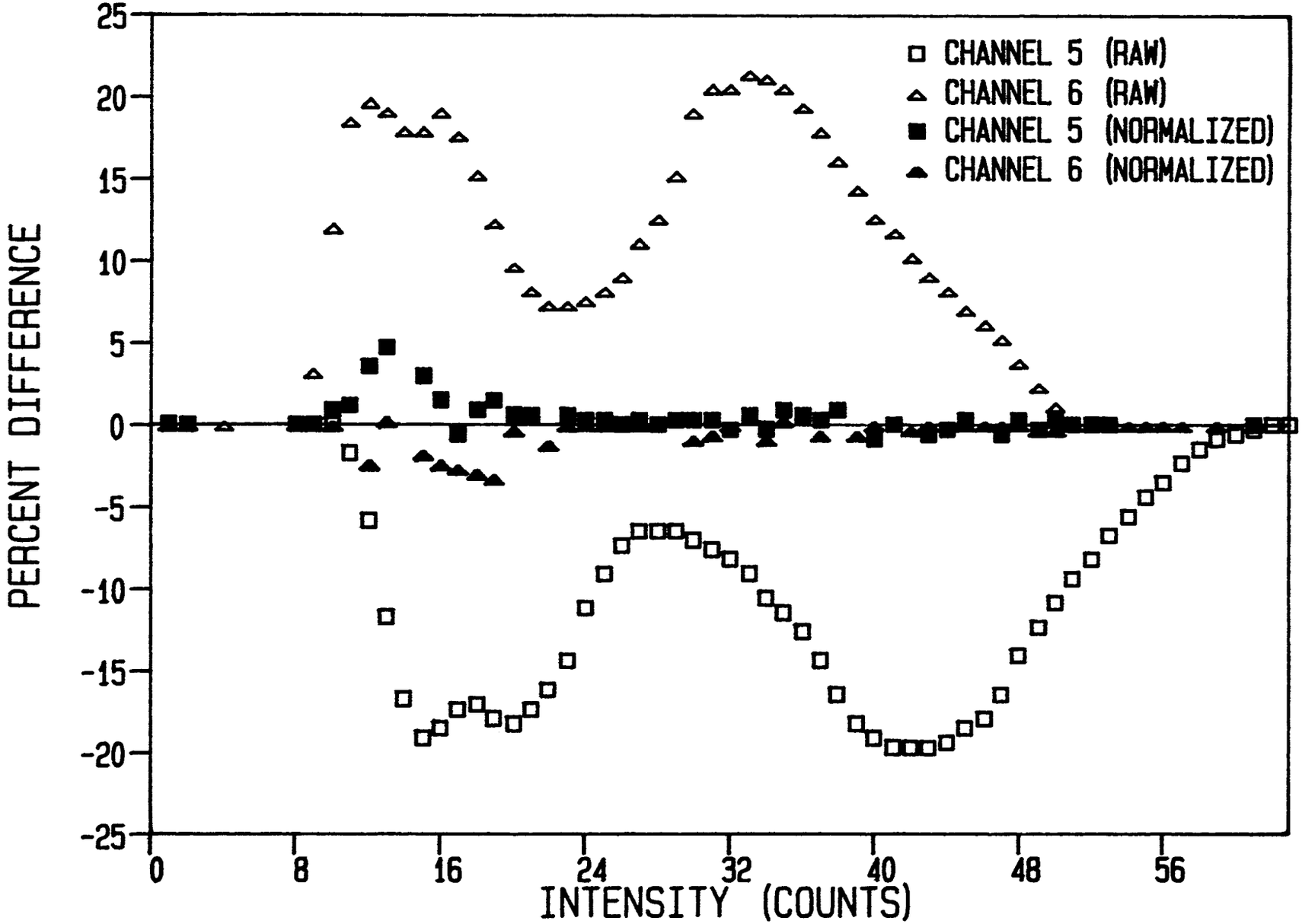

FIGURE 14. Percent differences for image data of June 1, 1988. Open symbols indicate unnormalized (raw) data; solid, normalized data.

APPENDIX. NORMALIZATION LOOK-UP TABLE

The normalization look-up table derived from the empirical distribution functions of May 18, 1988, is listed in Table 1. To find the normalized instrument output from a raw instrument output, one locates the raw intensity in the column labelled "Raw Counts" and reads across to the column for the appropriate channel under the label, "Normalized Counts in Channel". For example, in channel 6, for a raw output of 27 counts, the normalized output is 34 counts. Note that normalization is an identity operation in channel 2, since that channel is the reference channel.

TABLE 1. Normalization Look-Up Table from Data of May 18, 1988.

Raw	Normalized Counts in Channel							
Counts	1	2	3	4	5	6	7	8
0	0	0	0	0	0	0	0	0
1	1	1	1	1	1	1	1	1
2	2	2	2	2	2	2	2	2
3	3	3	3	3	3	9	3	3
4	4	4	4	4	4	9	4	4
5	5	5	5	5	5	9	5	5
6	6	6	6	6	6	9	6	6
7	7	7	7	7	7	9	7	7
8	8	8	8	8	8	10	8	9
9	9	9	8	9	8	12	9	9
10	10	10	8	11	8	13	10	11
11	12	11	9	12	9	15	11	12
12	13	12	10	13	9	16	12	13
13	14	13	10	14	10	17	13	14
14	14	14	11	15	10	18	14	15
15	15	15	12	16	11	19	15	16
16	16	16	14	17	12	20	16	17
17	17	17	15	19	13	22	17	18
18	18	18	16	20	15	23	18	19
19	19	19	17	21	15	24	19	21
20	20	20	17	22	16	25	20	22
21	21	21	18	23	17	26	22	23
22	22	22	19	24	18	27	23	24
23	23	23	19	26	18	28	23	25
24	24	24	21	27	19	30	24	26
25	25	25	21	28	20	31	25	27
26	26	26	23	29	21	32	26	28
27	27	27	23	30	23	34	28	29
28	28	28	24	31	23	35	28	30
29	29	29	25	33	24	37	29	32
30	30	30	26	34	25	39	31	33
31	31	31	27	36	26	40	32	34

TABLE 1 (CONTINUED)

Raw Counts	Normalized Counts in Channel 1	2	3	4	5	6	7	8
32	32	32	27	37	27	42	33	36
33	33	33	28	38	27	43	34	37
34	34	34	29	39	28	45	35	38
35	35	35	29	40	29	46	36	39
36	36	36	30	41	29	47	37	40
37	37	37	31	43	30	48	38	41
38	38	38	31	44	30	49	39	42
39	39	39	32	46	31	50	40	44
40	40	40	33	47	32	51	41	45
41	41	41	34	47	33	51	42	46
42	42	42	34	48	33	52	43	47
43	43	43	35	49	34	53	44	48
44	44	44	36	49	35	53	45	48
45	45	45	37	50	35	54	46	49
46	46	46	38	51	36	55	47	49
47	47	47	38	51	37	56	48	50
48	48	48	40	53	38	57	49	51
49	49	49	41	54	40	59	50	53
50	50	50	43	55	41	61	51	54
51	51	51	44	56	43	61	52	55
52	52	52	46	57	44	61	53	56
53	53	53	47	59	45	61	54	57
54	54	54	48	61	47	61	55	58
55	55	55	48	61	48	61	56	59
56	56	56	49	61	48	61	57	61
57	57	57	50	61	49	61	58	61
58	57	58	51	61	50	61	59	61
59	58	59	51	61	50	61	61	61
60	59	60	52	61	51	61	61	61
61	60	61	53	61	52	61	61	61
62	61	62	54	61	53	61	61	61
63	61	63	61	61	61	61	61	61

(Continued from inside front cover)

NESDIS 8 A Technique that Uses Satellite, Radar, and Conventional Data for Analyzing and Short-Range Forecasting of Precipitation from Extratropical Cyclones. Roderick A. Scofield and Leroy E. Spayd Jr., November 1984. (PB85 164994/AS)

NESDIS 9 Surface Cyclogenesis as Indicated by Satellite Imagery. Frank Smigielski and Gary Ellrod, March 1985. (PB85 191815/AS)

NESDIS 10 Detection of High Level Turbulence Using Satellite Imagery and Upper Air Data. Gary Ellrod, April 1985. (PB85 208452/AS)

NESDIS 11 Publications and Final Reports on Contracts and Grants, 1984. Nancy Everson, April 1985. (PB85 208460/AS)

NESDIS 12 Monthly Infrared Imagery Enhancement Curves: A Tool for Nighttime Sea Fog Identification off the New England Coast. E.M. Maturi and Susan J. Holmes, May 1985. (PB85 237725/AS)

NESDIS 13 Characteristics of Western Region Flash Flood Events in GOES Imagery and Conventional Data. Eric Fleming and Leroy Spayd Jr., May 1986. (PB86 209459/AS)

NESDIS 14 Publications and Final Reports on Contracts and Grants, 1985. Nancy Everson, June 1986. (PB86 232477/AS)

NESDIS 15 An Experimental Technique for Producing Moisture Corrected Imagery from 1 Km Advanced Very High Resolution Radiometer (AVHRR) Data. Eileen Maturi, John Pritchard and Pablo Clemente-Colon, June 1986. (PB86 24535/AS)

NESDIS 16 A Description of Prediction Errors Associated with the T-Bus-4 Navigation Message and a Corrective Procedure. Frederick W. Nagle, July 1986. (PB87 195913)

NESDIS 17 Publications and Final Reports on Contracts and Grants, 1986. Nancy Everson, April 1987. (PB87 220810/AS)

NESDIS 18 Tropical Cyclone Center Locations from Enhanced Infrared Satellite Imagery. J. Jixi, and V.F. Dorvak, May 1987. (PB87 213450/AS)

NESDIS 19 A Suggested Hurricane Operational Scenario for GOES I-M. W. Paul Menzel, Robert T. Merrill and William E. Shenk, December 1987. (PB88-184817/AS)

NESDIS 20 Satellite Observed Mesoscale Convective System (MCS) Propagation Characteristics and a 3-12 Hour Heavy Precipitation Forecast Index. Jiang Shi and Roderick A. Scofield, December 1987. (PB88-180161)

NESDIS 21 The GVAR Users Compendium (Volume 1). Keith McKenzie and Raymond J. Komajda (MITRE Corp.), May 1988. (PB88-241476)

NESDIS 22 Publications and Final Reports on Contracts and Grants, 1987. Nancy Everson, April 1988. (PB88-240270)

NESDIS 23 A Decision Tree Approach to Clear Air Turbulence Analysis Using Satellite and Upper Air Data. Gary Ellrod, January 1989.

NOAA SCIENTIFIC AND TECHNICAL PUBLICATIONS

The National Oceanic and Atmospheric Administration was established as part of the Department of Commerce on October 3, 1970. The mission responsibilities of NOAA are to assess the socioeconomic impact of natural and technological changes in the environment and to monitor and predict the state of the solid Earth, the oceans and their living resources, the atmosphere, and the space environment of the Earth.

The major components of NOAA regularly produce various types of scientific and technical information in the following kinds of publications:

PROFESSIONAL PAPERS—Important definitive research results, major techniques, and special investigations.

CONTRACT AND GRANT REPORTS—Reports prepared by contractors or grantees under NOAA sponsorship.

ATLAS—Presentation of analyzed data generally in the form of maps showing distribution of rainfall, chemical and physical conditions of oceans and atmosphere, distribution of fishes and marine mammals, ionospheric conditions, etc.

TECHNICAL SERVICE PUBLICATIONS—Reports containing data, observations, instructions, etc. A partial listing includes data serials; prediction and outlook periodicals; technical manuals, training papers, planning reports, and information serials; and miscellaneous technical publications.

TECHNICAL REPORTS—Journal quality with extensive details, mathematical developments, or data listings.

TECHNICAL MEMORANDUMS—Reports of preliminary, partial, or negative research or technology results, interim instructions, and the like.

U.S. DEPARTMENT OF COMMERCE
NATIONAL OCEANIC AND ATMOSPHERIC ADMINISTRATION
NATIONAL ENVIRONMENTAL SATELLITE, DATA, AND INFORMATION SERVICE
Washington, D.C. 20233